PRELIMINARY EXPERIMENTS WITH A CALIBRATION TECHNIQUE FOR GYRO AND DOPPLER NAVIGATION SENSORS FOR PRECISION UNDERWATER NAVIGATION

James C. Kinsey and Louis L. Whitcomb *
Department of Mechanical Engineering
The Johns Hopkins University
jkinsey@jhu.edu, llw@jhu.edu

Abstract

This paper addresses the calibration of bottom-lock Doppler sonar for the navigation of underwater robot vehicles. A least-squares *in-situ* method is reported for the estimation of the rotational alignment between a bottom-lock Doppler sonar and a gyroscope, employing sensors commonly used abroad underwater vehicles.

1 Introduction

This paper examines the problem of *in-situ* calibration of navigation sensor alignment parameters arising in the precision bottom-lock Doppler navigation of underwater vehicles. Previously reported studies by the authors and others have shown that the principal error sources arising in the Doppler navigation of underwater vehicles are (a) heading and attitude sensor accuracy and precision and (b) sensor rotation calibration (alignment) errors between the Doppler sonar and the attitude sensor [5, 19, 11]. Recently, a new class of low-cost, true-north seeking, 3-axis fiber-optic gyroscopes have become available. These new optical gyroscopes possess the ability to find true North at sea within about five minutes from a cold start, and provide a rated dynamic accuracy of 0.1° — about an order of magnitude better precision than the best available gyro-stabilized magnetic compasses, and is absolutely referenced to the geode. This new class of gyroscopes effectively solve problem (a), accuracy and precision, and in consequence problem (b), alignment and calibration, becomes the principal error source.

This paper proposes a method to experimentally identify sonar/gyro alignment rotation offsets employing only the sensors themselves and tracking information obtained from a commonly available long baseline (LBL) acoustic navigation system. The remainder of this section reviews the need for *in-situ* alignment calibration, the problem of underwater vehicle navigation, the specifics of Doppler sonar navigation, and previous work in Doppler navigation. Section 2 reports a method to directly compute sonar/gyro alignment calibration with experimental data from the sonar, gyro, and a LBL tracking system.

1.1 The Need for In-Situ Alignment Calibration

The *in-situ* alignment calibration problem for Doppler navigation arises because the Doppler sonar and heading/attitude sensor often must be placed in differing locations and orientations on an underwater vehicle. Although it would be desirable to "hard mount" the Doppler sensor directly to the attitude sensor, and to calibrate the alignment during manufacture, this is often impossible in practice.

This calibration problem first became apparent while implementing DVLNAV, a real-time

*We gratefully acknowledge the support of the National Science Foundation.

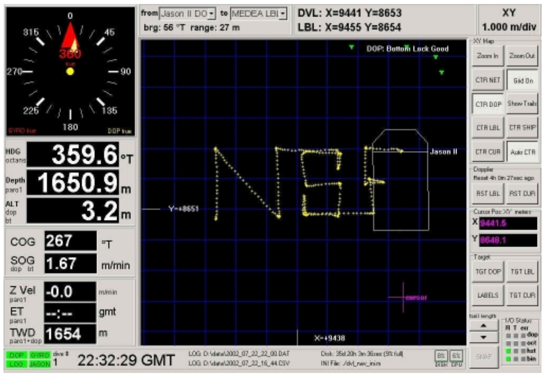

Figure 1: DVLNAV screen shot showing doppler-based navigation and closed-loop tracking performance of the new *Jason II* during Sea Trials on July 22, 2002 at 1650m depth on the Juan de Fuca Ridge.

vehicle navigation software package providing both long baseline navigation and combined Doppler/gyro navigation in a single application, Figure 1. Over the last three years, the authors and collaborators at the Woods Hole Oceanographic Institution (WHOI) have deployed DVLNAV to perform Doppler/gyro navigation on a variety of oceanographic vehicles, including the United Kingdom's *ISIS* ROV, the Institute for Exploration's *Hercules* ROV, and WHOI's *Jason II* ROV and inhabited deep-diving submersible *Alvin*. On all of these vehicles, the Doppler is mounted separately from the gyro. On *Alvin*, the Doppler is mounted on the tail-cone of the submarine, and the gyro is located 6.5 meters away — within the submarine's titanium passenger pressure sphere.

1.2 Review of Underwater Vehicle Navigation

At present, few techniques exist for reliable three-dimensional position sensing for underwater vehicles. Table 1 summarizes the sensors most commonly used to measure a vehicle's six degree-of-freedom position. While depth, altitude, heading, and attitude are instrumented with high bandwidth internal sensors, XY position sensing is usually achieved by acoustically interrogating fixed seafloor-mounted transponder beacons [9, 12].

Ultra-short baseline acoustic navigation systems are preferred for the task of docking a vehicle to a transponder-equipped docking station but are of limited usefulness for general long-range navigation [14, 15]. Inertial navigation systems offer excellent strap-down navigation capabilities, but are of limited utility in the low-speed low-acceleration regime typical for oceanographic robotic vehicles. Moreover, their high cost generally precludes their widespread use in civilian oceanographic instruments and vehicles. The U.S. sponsored Global Positioning System (GPS) provides superior three-dimensional navigation capability for both surface and air vehicles, and is employed by all U.S. oceanographic research surface vessels. The GPS system's radio-frequency signals are blocked by seawater, thus GPS signals cannot be directly received by deeply submerged ocean vehicles. Although recent work suggests that the next generation of acoustic communication networks might provide position estimation [7, 14], no systems providing this capability are commercially available at present.

The standard method for full ocean depth XYZ acoustic navigation is 12 kHz long baseline ("12 kHz LBL") acoustic navigation [9]. 12 kHz LBL typically operates at up to 10 Km ranges with a range-dependent precision of +/- 0.1 to 10 Meters and update rates periods as long as 20 seconds [9, 12]. The precision and update rate of LBL position fixes vary over several orders of magnitude depending on the acoustic frequency, range, and acoustic path geometry. LBL navigation accuracy and precision can be improved to some extent by careful application of Kalman or other filtering techniques [3, 18, 1].

At present, the best method for obtaining sub-centimeter XY position sensing is to employ a high-frequency (typically 300 kHz or greater) LBL system. Unfortunately, due to the rapid attenuation of higher frequency sound in water, high frequency LBL systems typically have a very limited maximum range. All absolute acoustic navigation methods require careful placement of fixed transponders (i.e. fixed or moored on the sea-floor [20], on the hull of

Table 1: Commonly Used Underwater Vehicle Navigation Sensors

INSTRUMENT	VARIABLE	INTERNAL	UPDATE RATE	PRECISION	RANGE	DRIFT
Acoustic Altimeter	Z - Altitude	yes	varies: 0.1-10Hz	0.01-1.0 m	varies	—
Pressure Sensor	Z - Depth	yes	medium: 1Hz	0.01%	full-ocean	—
Inclinometer	Roll, Pitch	yes	fast: 1-10Hz	$0.1°$ - $1°$	$+/-45°$	—
Magnetic Compass	Heading	yes	medium: 1-2Hz	$1-10°$	$360°$	—
Gyro (mechanical)	Heading	yes	fast: 1-10Hz	$0.1°$	$360°$	$10°/h$
Gyro RLG/FOG	Heading	yes	fast: 1-1600Hz	$0.0018°$	$360°$	$0.5°/h$
Gyro North Seeking	Heading, Pitch, Roll, $\ddot{x}$,ω	yes	fast: 1-100Hz	$0.1°$	$360°$	—
12 kHz LBL	XYZ Position	NO	varies: 0.1-1.0 Hz	0.01-10 m	5-10 Km	—
300 kHz LBL	XYZ Position	NO	1.0-5.0 Hz	+/-0.002 m	100 m	—
IMU	$\ddot{x}, \omega, \dot{\omega}$	yes	fast: 1-1000Hz	0.01m	—	1%
Bottom-Lock Doppler	$\dot{x}_{body}$	yes	fast:1-5Hz	0.01m	varies	1%

a surface ship [12], or on sea-ice [4]) and are fundamentally limited by the speed of sound in water — about 1500 Meters/Second.

To demonstrate the precision of 300 kHz LBL, the *JHUROV* was held immobile for 10 minutes, while the 300kHz LBL system computed the vehicle's position at an update rate of 2Hz. Figure 2, left, shows the position distribution for the 300 kHz LBL navigation system. The standard deviations of the vehicle's X and Y positions during the experiment were 6.752×10^{-4} meters and 7.035×10^{-4} meters, respectively.

Figure 2, right, shows data from a JASON survey in which vehicle fixes were obtained simultaneously using (a) 12 kHz LBL navigation and (b) 300 kHz LBL navigation. The data was obtained during survey operations during JASON dive #250, June 17, 1999, from 18:08Z to 19:34Z. The 12 kHz LBL update rate was 0.16 Hz (one fix every 6 seconds). The 300 kHz LBL update rate was 1.6 Hz (one fix every 0.6 seconds). The figure shows the corresponding error histogram of X and Y 12 kHz LBL errors in comparison to 300 kHz LBL. The data shows the 12 kHz LBL X and Y fixes to have zero mean and a standard deviation of 0.27 meter and 0.21 meter, respectively,

1.3 Notation

We employ the notation that a leading superscript indicates the frame of reference for a vector quantity, thus ${}^{w}\dot{p}_d(t)$, ${}^{v}\dot{p}_d(t)$, and ${}^{i}\dot{p}_d(t)$ represents the Doppler velocity in, respectively, the world, vehicle, and instrument frames of reference. A trailing subscript denotes the sensor source. Thus ${}^{w}\dot{p}_d(t)$ represents the Doppler velocity and ${}^{w}p_l(t)$ represents the LBL position, both in world coordinates. For rotation matrices, a leading superscript and subscript notation indicate the frames of reference. For example ${}^{w}_{v}R(t)$ is a rotation from the vehicle frame to the world frame, i.e. ${}^{w}\dot{p}_d(t) = {}^{w}_{v}R(t)\ {}^{v}\dot{p}_d(t)$.

We employ the standard notation $\otimes$ for the Kronecker product, and $(\cdot)^S$ for the stack (or vector) form of a matrix [8].

1.4 Doppler-Based UUV Navigation

Recently available bottom-lock Doppler sonars, typically work as follows: The Doppler transducer unit has four downward-looking beam transducers oriented at about 30° from the instrument vertical axis. A minimum of three beams are required; four are typically used.

The Doppler sensor measures the apparent bottom-velocity (due to the vehicle's motion) along each of the four beams. The velocity measurement in broadband Dopplers is performed with an ensemble of one or more discrete "pings" employing the entire set of four beams — this in contrast to some conventional Doppler techniques that employ continuous tones. The Doppler unit digitally processes the four ping responses to compute a 4×1 vector of velocities, $v_{beam}(t)$, representing the bottom velocity component along the respective beam axes. Single-ping velocity error standard-deviation varies with beam frequency. Velocity error standard-deviations vary with frequency and instrument design — our 1200 kHz unit provides a single-ping beam-velocity error standard deviation of 0.2%.

The 4×1 vector of beam radial velocities, $v_{beam}(t)$, is converted to the instrument-frame XYZ velocities, ${}^{i}\dot{p}_d(t)$, by the linear transformation

$$ {}^{i}\dot{p}_d(t) = T\ v_{beam}(t) \quad (1) $$

where the matrix T is a 3×4 constant matrix mapping the four beam velocities into a 3×1 vector of instrument velocities

$$ {}^{i}\dot{p}_d(t) = \begin{bmatrix} \dot{x}(t) \\ \dot{y}(t) \\ \dot{z}(t) \end{bmatrix} \quad (2) $$

representing the cartesian velocities $\dot{x}(t), \dot{y}(t)$, and $\dot{z}(t)$, in instrument-frame coordinates.

The instrument-frame velocity, ${}^{i}\dot{p}_d(t)$, is converted to the world-frame XYZ velocity, ${}^{w}v_d(t)$, by the linear transformation

$$ {}^{w}\dot{p}_d(t) = {}^{w}_{v}R(t)\ {}^{v}_{i}R\ {}^{i}\dot{p}_d(t) \quad (3) $$

where ${}^{w}_{v}R(t)$ is the time-varying rotation matrix from the vehicle frame to world frame, and ${}^{v}_{i}R$ is the constant rotation matrix from the Doppler sonar's instrument frame to the vehicle frame, referred to herein as the sensor alignment rotation matrix. The value of ${}^{w}_{v}R(t)$ is computed from heading, pitch, and roll values provided by the vehicle's 3-axis gyroscope. A method for the experimental determination of ${}^{v}_{i}R$ is the subject of this paper.

The world velocities, ${}^{w}\dot{p}_d(t)$, are integrated to compute bottom track position

$$ {}^{w}\hat{p}_d(t) = {}^{w}\hat{p}_d(t_0) + \int_{t_0}^{t} {}^{w}_{v}R(\tau)\ {}^{v}_{i}R\ {}^{i}\dot{p}(\tau)d\tau \quad (4) $$

where ${}^{w}\hat{p}_d(t)$ is the position estimate at time t as a function of the sensor signals and the initial position estimate ${}^{w}\hat{p}(t_0)$. For a more detailed discussion of the Doppler sensor equations and coordinate conversions, the reader is referred to [5, 13].

1.5 Previous Work

In [16] Spindel and colleagues report an acoustic navigation system combining LBL navigation techniques with transponder-based Doppler velocity sensing. In [5] Brokloff reports a bottom-lock doppler-based dead-reckoning system combining a 300kHz Doppler and an inertial navigation unit (for vehicle heading and attitude data) to obtain relative navigation errors of 0.4% of distance traveled over long (five hour) high-speed (five knot) missions. In [6] Brokloff extends the previous results to employ water-lock Doppler tracking when the vehicle altitude exceeds bottom-lock range.

In [20] the authors report preliminary results from the first deployment of the combined LBL/Doppler navigation system described herein. In [19] the authors identify principal limitations to the bottom-track precision of Doppler based navigation systems and analyze the effect of heading-sensor errors on doppler bottom-track precision. The authors reported a new Doppler navigation system and further studied the effect of heading-sensor errors on Doppler bottom-track precision in [11]. In [10], the authors proposed a technique for *in-situ* calibration and presented simulation results.

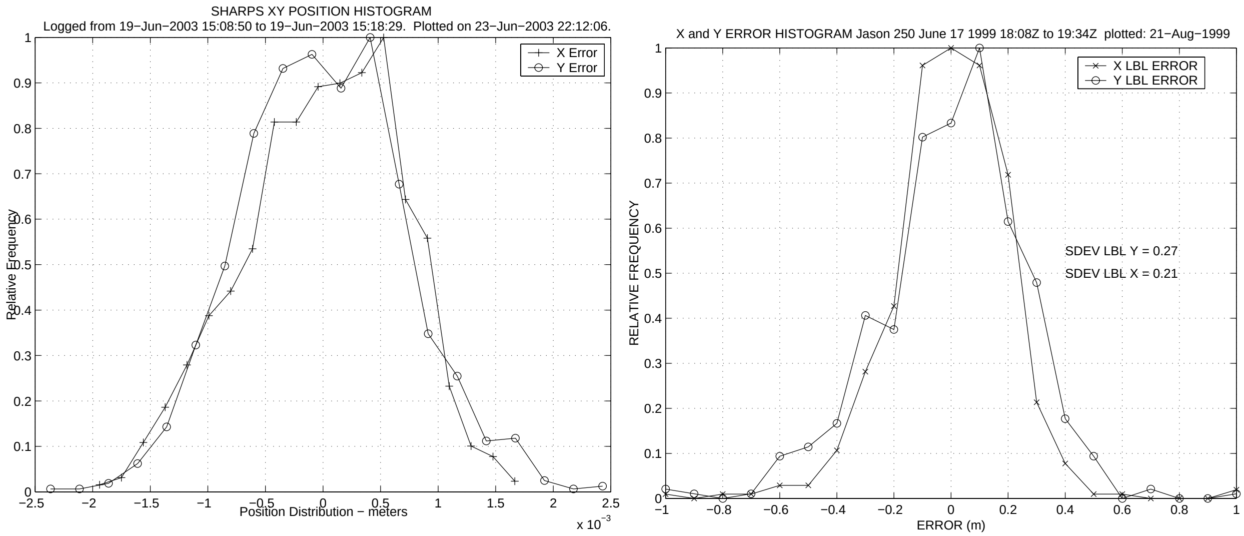

Figure 2: LBL navigation precision: Left, histogram plot of a 300kHz navigation system used aboard the *JHUROV*. XY standard deviations are 6.752x10^{-4} meters and 7.035x10^{-4} meters, respectively. Right, a histogram plot of the LBL tracking errors during closed-loop survey operations on JASON dive #250 June 17 1999 18:08Z to 19:34Z. XY standard deviations are 0.21 meters and 0.27 meters, respectively.

2 The Alignment Calibration Problem

The remainder of this paper addresses the following *in-situ* doppler-gyroscope alignment calibration problem: Consider a vehicle possessing the following three navigation sensors:

1. A bottom-lock Doppler providing 3-axis translational velocities, ${}^{i}\dot{p}_d(t_i)$ in instrument coordinates. Good commercially available units provide velocity measurements with single-ping standard deviations of 0.2% with update rates up to about 5 Hertz. The sensor alignment rotation matrix ${}^{v}_{i}R$ is constant but unknown.

2. A 3-axis north-seeking gyroscope providing absolute gyroscope attitude, ${}^{w}_{v}R(t_j)$, and attitude rate, ${}^{w}_{v}\dot{R}(t_j)$, with respect to true north and the local gravitational field. Good commercially available units provide dynamic 3-axis attitude at up to about 100 Hz.

3. A LBL acoustic navigation system providing absolute vehicle XYZ position measurements, ${}^{w}p_l(t_k)$ at relatively low update rates. Good commercially available systems provide absolute precision of 0.1 to 10 meters with update rates varying from 1.0 to 0.05 Hertz.

Our goal is to employ these sensor signals to experimentally determine an estimate ${}^{v}_{i}\hat{R}$ of the unknown sensor alignment rotation matrix ${}^{v}_{i}R$. Once ${}^{v}_{i}\hat{R}$ is known, the Doppler and gyro signals can accurately determine the vehicle position with the usual dead-reckoning algorithm (4). In the context of at-sea underwater vehicle operations, this calibration procedure would normally be employed when the sensors are first installed on a vehicle, or when the sensor mounting positions are altered for maintenance or operational purposes.

For simplicity of exposition, assume that (a) the LBL transponder is co-located with the Doppler transducer at the origin of the vehicle's reference frame and (b) the coordinate axes of the vehicle frame are defined as the coordinate axes of the gyro. While these assumptions greatly simplify the navigation equations for clarity of exposition, they can easily be relaxed without requiring any fundamental change in the proposed methodology.

Note that in this section we employ continuous time notation despite the fact that these sensors actually provide asynchronous sensor readings at discrete intervals of varying period. While it might at first appear attractive to immediately adopt a discrete-time representation in order to more closely correspond to the actual discretely sampled sensor signals, this task is complicated by the fact that these sensors operate asynchronously, provide data at independently differing intervals, and cannot be exactly synchronized to a single fixed sample interval. In consequence, we adopt the theoretically unjustified but common practice of employing continuous-time mathematical analysis, and an *ad-hoc* discrete-time implementation. Although the discrete-time implementation is only an approximation of the continuous time system, the sequel shows that the discrete time system results agree favorably with those predicted by analysis of the exact continuous time system.

2.1 Least-Squares Alignment Calibration

A first, direct method to solve for the unknown constant rotation matrix ${}^{v}_{i}R$ in (4) takes advantage of the fact that ${}^{v}_{i}R$ enters linearly into (4). Applying the identity $(ABC)^S = (C^T \otimes A)B^S$ to (4) results in

$$ {}^{w}\hat{p}(t) = \int_{t_0}^{t} [\ {}^{i}\dot{p}^T(\tau) \otimes\ {}^{w}_{v}R(\tau)]d\tau(\ {}^{v}_{i}R)^S \qquad (5)$$

which can be solved for the unknown vector $(\ {}^{v}_{i}R)^S$ by any standard method for solving overdetermined linear systems (for example the standard Moore-Penrose inverse) over any interval $[t_0, t]$ for which ${}^{i}\dot{p}(t)$ exhibits persistent excitation, i.e. when

$$\int_{t_0}^{t}\ {}^{i}\dot{p}(\tau)\ {}^{i}\dot{p}^T d\tau \qquad (6)$$

is full rank. The disadvantage of this direct method is that the general Moore-Penrose solution is only guaranteed to compute a ${}^{v}_{i}R \in SO(3)$ only in the zero-noise case.

A second, alternative, method is to solve the velocity equation (3) for ${}^{v}_{i}R\ {}^{i}\dot{p}(t)$ thus

$$ {}^{v}_{w}R(t)\ {}^{w}\dot{p}(t) = {}^{v}_{i}R\ {}^{i}\dot{p}(t). \qquad (7)$$

The relation (7) can be solved directly for the unknown rotation matrix ${}^{v}_{i}R$ over any interval for which ${}^{i}\dot{p}^T(\tau)$ exhibits persistent excitation. The fatal disadvantage of this second method is that the signal $\dot{p}(t)_w$ is not available in practice. In actual LBL systems, the world position measurement ${}^{w}p_l(t)$ is provided only at lengthy discrete intervals (typically 1 to 20 second periods), and the measurement signal contains sufficient noise as to render numerical differentiation useless.

We propose a third, practical approach. Both sides of (7) are integrated to obtain

$$ {}^{v}_{w}\int R(\tau)\ {}^{w}\dot{p}_l(\tau)dt = {}^{v}_{i}R\int\ {}^{i}\dot{p}(\tau)_d dt. \qquad (8)$$

Integrating the left hand side by parts to eliminate the unavailable $\dot{p}(t)_w$ signal results in

$$ \begin{aligned} {}^{v}_{w}R(t)\ {}^{w}p_l(t) - \int\ {}^{v}_{w}\dot{R}(\tau)\ {}^{w}p_l(\tau)d\tau \\ = {}^{v}_{i}R\int\ {}^{i}\dot{p}_d(\tau)d\tau \end{aligned} \qquad (9)$$

which only depends on readily available signals: the raw Doppler instrument velocity signals ${}^{i}\dot{p}_d(t_i)$, the raw gyro angular position ${}^{v}_{w}R(t_j)$ and angular velocity ${}^{v}_{w}\dot{R}(t_j)$, and the world-referenced LBL position ${}^{w}_{i}p_l(t)$. The expression (9) can be solved for the unknown rotation matrix ${}^{v}_{i}R$ over any interval for which ${}^{i}\dot{p}_d$ exhibits persistent excitation. Two methods are commonly employed to solve equations of this form. If we define

$$ \begin{aligned} \alpha(t) &= {}^{v}_{w}R(t)\ {}^{w}p_l(t) - \textstyle\int_{t_0}^{t}\ {}^{v}_{w}\dot{R}(\tau)\ {}^{w}p_l(\tau)d\tau \\ \beta(t) &= \textstyle\int_{t_0}^{t}\ {}^{i}\dot{p}_d(\tau)d\tau \end{aligned} \qquad (10)$$

then (9) can be written

$$\alpha(t) = {}^{v}_{i}R\,\beta(t) \qquad (11)$$

which can be solved for ${}^{v}_{i}R$ by the standard Moore-Penrose inverse

$$ {}^{v}_{i}R^T = \int_{t_0}^{t}\beta(\tau)\alpha(\tau)^T d\tau[\int_{t_0}^{t}\beta(\tau)\beta(\tau)^T d\tau]^{-1}. \qquad (12)$$

As in the previous cases, the Moore-Penrose inverse solution computes a ${}^{i}_{v}R \in SO(3)$ only in the zero-noise case. Alternatively, the singular value decomposition (SVD) approach originally reported in [2] provides a least square solution subject to the additional constraint that ${}^{i}_{v}R \in SO(3)$. The reader is referred to [2, 17] for a detailed exposition of the SVD solution method.

3 Performance Evaluation

3.1 Simulation Performance

In [10], we report the results of simulation studies examining the performance of the proposed calibration method. The results indicate satisfactory performance of the proposed method in the presence of simulation noise.

3.2 Experimental Performance

We are presently conducting trials with the *JHUROV* to experimentally evaluate the performance of the proposed method, and expect to report these results at the workshop.

4 Conclusions

This paper identified a practical problem arising in the calibration of bottom-lock Doppler sonar for the navigation of underwater vehicles. A least-squares *in-situ* method is reported for the estimation of the rotational alignment between a bottom-lock Doppler sonar and a gyroscope, employing sensors commonly used abroad underwater vehicles.

Acknowledgements

We are grateful to the Deep Submergence Operations Group (DSOG) at the Woods Hole Oceanographic Institution (WHOI) for their ongoing collaboration in developing and fielding these new navigation systems in support of oceanographic science.

References

[1] P. E. An, A. J. Healey, J. Park, and S. M. Smith. Asynchronous data fusion for AUV navigation via heuristic fuzzy filtering techniques. In *Proceedings of IEEE Oceans'97*, pages 397–402, October 1997.

[2] K. S. Arun, T. S. Huang, and S. D. Blostein. Least-squares fitting of two 3-D point sets. *IEEE Transactions on Pattern Analysis and Machine Intelligence*, PAMI-9(5):698–700, 1987.

[3] B. M. Bell, B. M. Howe, J. A. Mercer, and R. C. Spindel. Nonlinear kalman filtering of long-baseline, short-baseline, GPS, and depth measurements. In *Conference Record of the Twenty-Fifth Asilomar Conference on Signals, Systems and Computers*, pages 131–136, Pacific Grove, CA, USA, November 1991.

[4] J. G. Bellingham, M. Deffenbaugh, J. Leonard, and J. Catipovic. Arctic under-ice survey operations. *Unmanned Systems*, 12(1):24–9, 1994.

[5] N. Brokloff. Matrix algorithm for Doppler sonar navigation. In *Proceedings of IEEE/MTS OCEANS'94*, volume 2, pages 378–83, September 1994.

[6] N. Brokloff. Dead reckoning with an ADCP and current extrapolation. In *Proceedings of IEEE/MTS OCEANS'97*, volume 2, pages 994–1000, October 1997.

[7] J. A. Catipovic and L. E. Freitag. High data rate acoustic telemetry for moving ROVs in a fading multipath shallow water environment. In *Proceedings of the Symposium on Autonomous Underwater Vehicle Technology. AUV '90*, pages 296–303, 1990.

[8] A. Graham. *Kronecker Products and Matrix Calculus With Applications*. Halsted Press,John Wiley and Sons, NY, 1981.

[9] M. M. Hunt, W. M. Marquet, D. A. Moller, K. R. Peal, W. K. Smith, and R. C. Spindell. An acoustic navigation system. Technical Report WHOI-74-6, Woods Hole Oceanographic Institution, Woods Hole, Massachusetts 02543 USA, December 1974.

[10] J. C. Kinsey and L. L. Whitcomb. Towards in-situ calibration of gyro and Doppler navigation sensors for precision underwater vehicle naviagation. In *Proceedings of IEEE ICRA 2002*, volume 4, pages 4016–4023, MAY 2002.

[11] J. C. Kinsey and L. L. Whitcomb. Preliminary field experience with the DVLNAV integrated navigation system for manned and unmanned submersibles. In *Proceedings of the 1st IFAC Workshop on Guidance and Control of Underwater Vehicles*, pages 83–88, April 2003.

[12] P. H. Milne. *Underwater Acoustic Positioning Systems*. Gulf Publishing, Houston, 1983.

[13] RD Instruments Inc. ADCP coordinate transformations. Technical Report P/N 951-6079-00, RD Instruments Inc, 9855 Businesspark Avenue, San Diego, California, 92131, April 1997.

[14] H. Singh, J. Catipovic, R. Eastwood, L. Freitag, H. Henricksen, F. Hover, D. Yoerger, J. Bellingham, and B. Moran. An integrated approach to multiple AUV communications, navigation and docking. In *Proceedings of the OCEANS 96 MTS/IEEE Conference*, pages 59–64, Fort Lauderdale, FL, USA, September 1996.

[15] S. M. Smith and D. Kronen. Experimental results of an inexpensive short baseline acoustic positioning system for AUV navigation. In *Proceedings of IEEE Oceans'97*, pages 714–720, October 1997.

[16] R. C. Spindel, R. P. Porer, W. M. Marquet, and J. L. Durham. A high-resolution pulse-Doppler underwater acoustic navigation system. *IEEE Journal of Oceanic Engineering*, 1(1):6–13, September 1976.

[17] S. Umeyama. Least-squares estimation of transformation parameters between two point patterns. *IEEE Transactions on Pattern Analysis and Machine Intelligence*, PAMI-13(4):376.380, 1991.

[18] J. Vaganay, J. G. Bellingham, and J. J. Leonard. Comparison of fix computation and filtering for autonomous acoustic navigation. *International Journal of Systems Science*, 29(10):1111–22, October 1998.

[19] L. L. Whitcomb, D. R. Yoerger, and H. Singh. Advances in Doppler-based navigation of underwater robotic vehicles. In *Proceedings of the IEEE International Conference on Robotics and Automation*, May 1999.

[20] L. L. Whitcomb, D. R. Yoerger, H. Singh, and D. A. Mindell. Towards precision robotic maneuvering, survey, and manipulation in unstructured undersea environments. In Y. Shirai and S. Hirose, editors, *Robotics Research - The Eighth International Symposium*, chapter 2, pages 45–54. Springer-Verlag, London, 1998.